Water-Based Robotic Fabrication: Large-Scale Additive Manufacturing of Functionally Graded Hydrogel Composites via Multichamber Extrusion

Laia Mogas-Soldevila,[1,*] Jorge Duro-Royo,[1,*] and Neri Oxman[1]

Abstract

Additive manufacturing (AM) of regenerated biomaterials is in its infancy despite the urgent need for alternatives to fuel-based products and in spite of the exceptional mechanical properties, availability, and biodegradability associated with water-based natural polymers. This study presents water-based robotic fabrication as a design approach and enabling technology for AM of biodegradable hydrogel composites. Our research focuses on the combination of expanding the dimensions of the fabrication envelope, developing structural materials for additive deposition, incorporating material-property gradients, and manufacturing architectural-scale biodegradable systems. This work presents a robotically controlled AM system to produce biodegradable-composite objects combining natural hydrogels, such as chitosan and sodium alginate, with other organic aggregates. It demonstrates the approach by designing, building, and evaluating the mechanics and controls of a multichamber extrusion system. Finally, it provides evidence of large-scale composite objects fabricated by our technology that display graded properties and feature sizes ranging from micro- to macroscale. Fabricated objects may be chemically stabilized or dissolved in water and recycled within minutes. Applications include the fabrication of fully recyclable products or temporary architectural components such as tent structures with graded mechanical and optical properties. Proposed applications demonstrate environmental capabilities such as water-storing structures, hydration-induced shape forming, and product disintegration over time.

Introduction

The use of regenerated biomaterials for large-scale architectural and engineering applications is in its infancy despite an urgent need for alternatives to fuel-based plastic materials as petroleum supply decreases. This is in spite of the fact that natural materials display exceptional mechanical properties such as those of wood with strength comparable to steel, shell with higher toughness than engineered ceramics, and bamboo with slenderness not yet generally achieved by modern engineering systems.[1,2,3] Natural polymers and polysaccharides, such as chitin, starch, cellulose, and hemicelluloses, provide for a vast renewable resource, produced by earth at rates much higher than human-made synthetic polymers. Polysaccharides, for example, can carry out multiple functions and typically display high levels of structural and functional diversity. Those include gel-forming properties displayed by agar and pectin, storage capabilities in starch and glycogen, as well as structural capabilities in cellulose and chitin. Capable of

[1]Mediated Matter Group, Media Lab, Department of Architecture and Urban Planning, Massachusetts Institute of Technology, Cambridge, Massachusetts.
*These two authors contributed equally to this work.

replacing existing synthetic polymers as well as providing new property combinations for relevant applications, their derivatives are likely to play a key role.[3,4]

Recent research in tissue engineering proves that biodegradable scaffolds from chitosan—deacetylated chitin from ground shrimp shells, a by-product of the fishing industry—and sodium alginate—a gum extracted from the cell walls of abundant brown algae—show significantly improved mechanical and biological properties.[5,6] Moreover, it has been shown that chitosan enables the manufacturing of medium three-dimensional (3D) objects, thereby offering a new pathway for large-scale production of fully compostable engineered components with complex forms. Recent developments deploy conventional manufacturing methods such as injection casting into epoxy resin molds to produce chitosan-based functional 3D industrial products, such as fully compostable cups and egg-storing containers.[1,2,7]

We present water-based robotic fabrication as an enabling technology for additive manufacturing (AM) of biodegradable hydrogel composites through an extrusion system that can produce large-scale 3D shapes and objects omitting the need of molds. This allows achieving a wide range of geometrical forms combining varying hydrogel and aggregate concentrations in the design of functional gradients. We employ volume-driven extrusion combined with high-capacity repositories converging into a single nozzle. Composites can be premixed and extruded, or mixed statically at the nozzle on-the-fly, achieving a wide range of material composition and enabling the deposition of functional material gradients.

By implementing a low-operation-energy open-ended extrusion system we can control the mixtures of diverse materials without the need for special formulations or specific physical forms such as the ones required by other AM processes, including photo-curing resins for stereolithography, powders or pellets for selective laser sintering (SLS), or filaments for fused deposition modeling (FDM). The large-scale bioplastic forms we produced display structural properties, functional mechanical gradients, and material features ranging from micro- to macroscale. These structures can be dissolved in water and recycled within minutes. Alternatively, they can be chemically stabilized to moisture and utilized to fabricate temporary architectural components with environmental functionalities such as water storage, hydration-induced shape changes, or nutrient release while biodegrading.

The Role of Water

In nature, water acts as an "invisible" support and shape-forming system. Its function is to mediate between internal chemical processes and external environmental stimuli.[8] It assembles basic molecules into structures with complex functions and property gradients such as the one found in the beak of the *Dosidicus gigas* squid where the water content contributes to the stiffness gradient.[8,9] The squid's beak is one of the hardest and stiffest wholly organic materials known, and in its internal structure, water and chitin negotiate generating exceptional material properties. Once hydrated, this material system exhibits a two-order-of-magnitude stiffness gradient.[9] Water is at the core of all biological materials: without it, polysaccharides such as chitin or chitosan would remain brittle.[4] Chitin is the second most important natural polymer in the world.[3,10] It can be found in many organisms such as crabs, lobsters, shrimp, mollusks, and octopi.[2,7]

In our research we focus on chitosan, as it is soluble in water; its concentrations can be tuned to additively manufacture functional gradients. Chitosan is produced industrially by de-acetylating chitin from 95% to 75%, and it appears naturally as part of the wall of several fungi. It is a natural linear polysaccharide with a hydrophilic surface, and unlike synthetic polymers it absorbs water. The presence of water modifies the mechanical properties of chitosan by separating its polymer charged groups inducing macrolevel softness, thereby producing an extrusion-compatible hydrogel.[7] Chitosan is a binder used as a resin matrix for industrial fiber-based composites. We find its workability—its mechanical and water-storing properties present in its various states—suitable for the deposition of structurally graded biodegradable composites.

Large-Scale AM

While industrial manufacturing has for decades focused on subtractive technologies, carving parts out of raw materials, nature employs additive strategies to form diverse and complex structures. AM enables the generation of 3D physical objects out of 3D digital models through the deposition of material in a layer-by-layer fashion. Despite the ability provided by AM to print highly complex geometrical forms, a print's envelope is generally confined by the print s tray size defining the deposition area in the *X* and *Y* dimensions. This is one of AM's main limitations.[11] Various projects in academia and industry are overcoming this limitation by designing large-scale gantries with increased surface area.

Oak Ridge National Laboratory (U.S. Department of Energy) is developing a "big area AM" technology that accommodates a cluster of coordinated robots operating in open-air environments to produce components and structures boundless in size.[12] Voxeljet (Germany) developed a continuous powder bed system (VXC800) enabling the production of unbounded parts along a single dimension.[13] The D-Shape 3D printer by Monolite Ltd. (Enrico Dini) has a 6000-mm-by-6000-mm aluminum frame with a printer head including 300 nozzles.[14] Commercial systems such as Objet1000 by Stratasys (S. Scott Crump) provide wide-format industrial-size models and 1:1 scale prototypes with a large build tray of 1000 mm by 800 mm by 500 mm.[15] By overcoming the envelope size limitation of AM, full-size structures could be manufactured at once enabling the fabrication of large-scale complex shapes and material properties within a single build that cannot be achieved with traditional AM technologies.

Structural AM

Structural biomaterials, such as cotton, silk, chitin, cellulose, coral, and even organs and cells, demonstrate remarkable

mechanical properties due to sophisticated internal organization of their building blocks.[3] Inspired by some of these natural materials and their structural mechanisms, research into AM and 3D printing is evolving toward incorporating sophisticated materials and material organization methods within the fabrication process.[11] While AM is typically deployed to rapidly fabricate prototypes of nonstructural materials, current research explores the use of AM for real-world applications by suggesting that structural materials can be 3D-printed in high resolution.[16] Companies and research groups that are at the forefront of this research appear to be growing incrementally: Oxford Performance Materials has developed an engineering resin for 3D printing with high mechanical strength, heat resistance. and biocompatibility properties[16]; Stratasys uses standard and engineering-grade thermoplastic filaments, such as tough nylon, to produce functional parts. The company has recently launched its PolyJet Objet500 Connex3 printer, known to be the first multicolor/multimaterial 3D printer with materials displaying excellent mechanical properties such as tensile strength, elongation at break, and multiple hardness values[15]; MarkForged has developed a method to 3D-print carbon-fiber and tough plastic reinforced composites.[16]

In the realm of sophisticated material organization, researchers at the Computational Synthesis Lab headed by Prof. Hod Lipson (Cornell University) have been investigating voxel-based multimaterial 3D printing since 2007.[17] Inspired by DNA, where a complex structure is formed from a discrete number of aligned building blocks, digital discrete matter explores massively parallel assembly of microscale units to achieve high dimensional accuracy, perfect repeatability, and the capability of low-temperature co-fabrication using a rich and diverse set of materials.[17] More recently, AM with metal has become possible, inspired by manual spray welding[16]; NASA is deploying a technique called selective laser melting with great success in the construction of steel-made rocket motor components,[18] and Arup (design engineering firm) has initiated a design method to 3D-print critical structural steel elements with a similar process.[19] Advances in structural material deposition enable the use of real-world materials with exceptional properties and renders AM a viable and promising manufacturing technology that goes well beyond prototyping.

Graded AM

Functionally graded materials (FGM) are human-made materials characterized by property variation. Triggered by position-dependent chemical composition, microstructure, or atomic order, such materials demonstrate high levels of anisotropic control.[20] The manufacturing process of FGM typically includes two stages: the creation of a spatial heterogeneous structure and its consolidation.[20] Gradients are obtained with constitutive, homogenizing, and segregating methods.[20] Consolidation is obtained by drying, sintering, or solidification techniques.[20] Recent advances in automation are making both gradation and consolidation processes technologically and economically viable.[20] In the fields of architecture, engineering, and product design, property gradation of single materials with multiple functions holds the potential to revolutionize how products and buildings are form-found, designed, and fabricated.[11] Ultimately, such advances will lead the way toward the design of multifunctional material systems with variable properties reducing the need for complex assembly of multiple parts with homogeneous properties and discrete functionality. This approach is inspired by the biological world where single-material systems are known to vary their internal composition in order to accommodate a variety of structural and environmental requirements manifested in stiffness gradients observed in the *Dosidicus gigas* squid's beak,[9] skin pores, tree structures,[3] or a silkworm's cocoon.[21]

Hydrogel AM

For the past decade, AM of hydrogels has become a rapidly evolving technique to produce nanofeatured biocompatible tissue scaffolds for tissue engineering purposes.[5,6,22,23] There are mainly three different biofabrication techniques known to achieve fully interconnected soft-material 3D structures, namely, laser-based, nozzle-based (also known as robotic dispensing), and printer-based (also known as inkjet printing) systems.[24,25] The fabrication of hydrogel scaffolds requires mild processing conditions. Therefore, AM techniques such as FDM or SLS cannot be used as they generally involve harsh processing conditions. With the exception of SLS, all the laser-based systems are suitable for hydrogel processing.[25] However, since the technique requires light energy to pattern materials, only photo-cross-linkable polymers are suitable for obtaining a cross-linked hydrogel network.[25]

Nozzle-based or robotic dispensing techniques involving elevated temperatures such as FDM are undesirable, but can be overcome by applying a mild dissolution process, benefiting the processing of hydrogels.[25] Pressure-actuated, solenoid-actuated, piezoelectric, and volume-actuated nozzles are the main nozzle types implemented as nozzle-based strategies for the deposition of hydrogels.[25] Small-scale commercially available nozzle-based systems for 3D dispensing include 3D-Bioplotter (EnvisionTEC), which can print a viscous material in a liquid one with a matching density and also tune strand thickness by altering viscosity, deposition speed, nozzle diameter, or pressure.[25] The system provides liquid flow with a pneumatic nozzle (using air pressure) or with a volume-driven nozzle (using a stepper motor).[25] More recently, open-source low-budget nozzle-based hydrogel-compatible systems are under development. One of the most successful systems characterized by high modifiability as well as a wide range of different tool heads is the Fab@Home project[26] developed by the Creative Machines Lab at Cornell University. The system consists of entirely off-the-shelf chassis, tool heads, and electronics. One of its hydrogel extrusion heads is actuated by a noncaptive motor direct-drive system[26] with a design strategy similar to the one presented here.

Printer-based systems implement inkjet technology through drop-on-demand or continuous ejection types.[25] As in nozzle-based systems, construct deposition occurs in an additional computer-

controlled, layer-by-layer sequence coupled with the deposition of material. The most relevant printer-based technology is 3DP™ developed by MIT Prof. Sachs[25]; this is the only solid-phase rapid-prototyping technology that is compatible with hydrogel manufacturing. The 3DP process consists of multiple cycles: first, a platform moves one layer down, then a roller spreads polymer powder into a thin layer, and finally an inkjet print-head sprays a liquid binder that bonds the powder particles together. All the hydrogel AM approaches mentioned above are known to produce small-scale biocompatible parts or scaffolds for bioengineering purposes. We are inspired by low-energy and mild-condition deposition systems in order to design large-scale functionally graded structures with environmental capabilities for applications in architectural and product design.

A Multichamber Extrusion System

Design Analysis

The designed system is portable with an overall weight of 4 kg, including loaded syringes and deposition material, and can be attached to an existing numerically controlled platform. Typical flow rates range from 8 to 4000 mm^3/sec, while linear motion varies between 10 and 50 mm/sec; nozzle sizes range from 0.5 to 8 mm inner diameter. The dispensing head moves in three dimensions, within the robotic arm envelope, while the fabrication platform is stationary. The dimensional limits of the process, when using a Kuka Agilus KR1100, are 1000 mm in length and 500 mm in width in order to deposit rectangular constructs. The portable extrusion system can be mounted on robotic arms with a larger envelope or other CNC machines. Figure 1 demonstrates the mechanical experimental setup.

Dimensioning Tests

Key experiments executed in the design of the extrusion system were performed using an Instron mechanical tester and a shear measurement AR-G2 viscometer (see Materials and Methods for further detail). From the initial testing, we obtained a 60 N axial load required to extrude the colloids from a 200 cc syringe

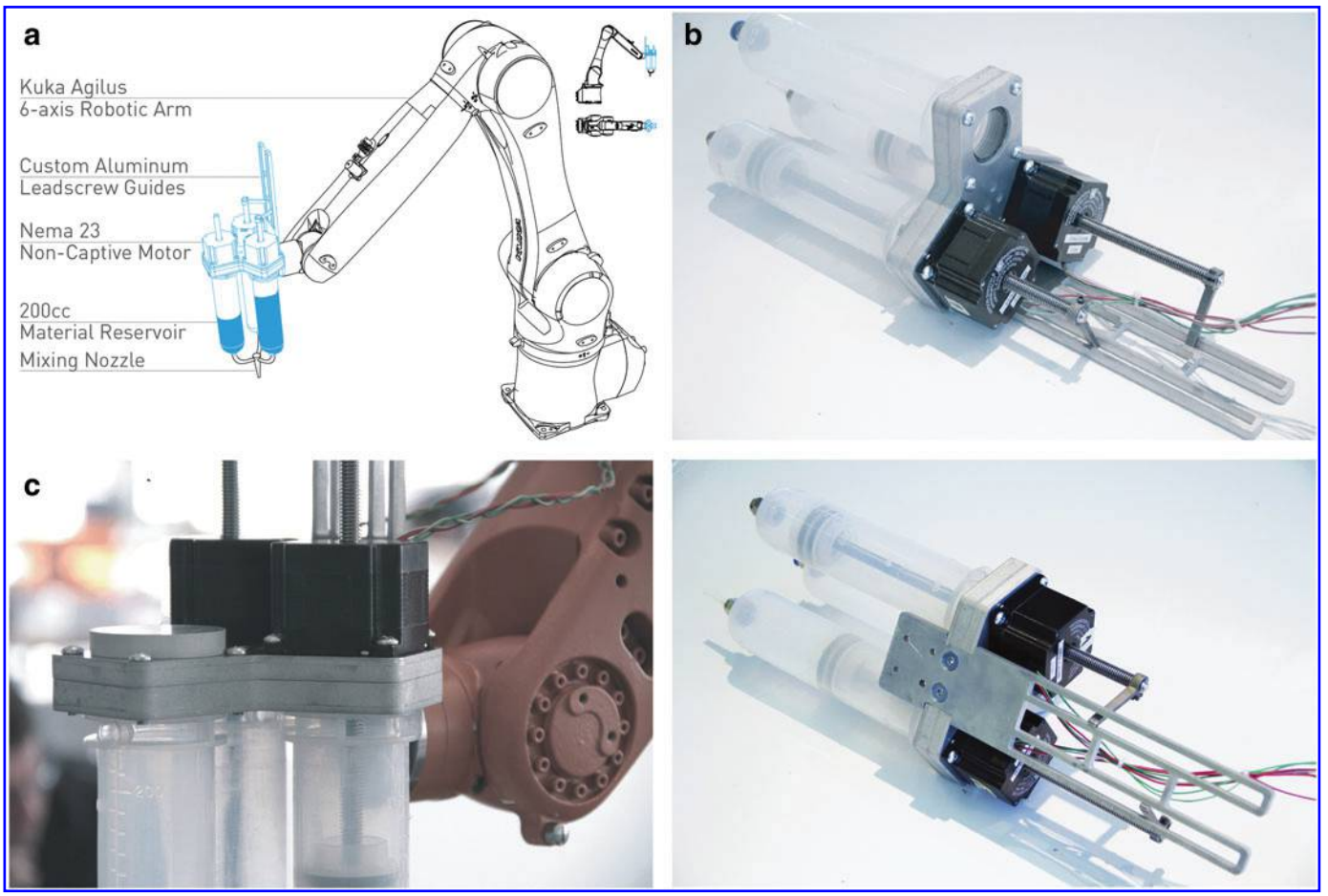

Figure 1. **(a)** Experimental setup: custom-designed portable multichamber extrusion system mounted as an end-effector of a Kuka KR AGILUS robotic arm (KR 10 R1100 SIXX WP). **(b)** Robotic end-effector with mounted extrusion system. **(c)** Front and side view of the three-chamber extrusion system with direct actuation of the plungers mounted on aluminum water-jet-cut plates allowing for deployment and replacement of custom nozzle tips. Color images available online at www.liebertpub.com/3dp

with a 0.7 mm nozzle, and we calculated a motor torque for direct drive of 1.8 Nm. In terms of travel speed, a maximum robotic arm end-effector displacement of 50 mm/sec was required in order to ensure proper extrusion of the materials (Figure 2a, c). Colloids tested under shear rates of 1–100 Pa over 10 min display properties that favor extrusion of the material, due in part to the presence of the sodium alginate additive in the chitosan matrix.[23] These favorable properties are due to the enhanced shear thinning behavior that sodium alginate provides, where the viscosity of the fluid decreases when the shear stress applied is increased. This change in the properties of the material is caused by shear-induced reorganization of the polymer chains to a more stretched conformation, which leads to decreased entanglement. For fabrication purposes, this implies a decreased shear stress at the high shear rates that are present inside a nozzle, followed by a sharp increase in viscosity upon deposition, facilitating the extrusion and printing fidelity of the viscous matrix.[23,24] We have chosen a concentration of sodium alginate of 3% w/v for sample production (Figure 2b).

Experimental Setup

Existing motion platform The extrusion system was attached to an existing motion platform's end-effector, a Kuka Agilus 6-axis robotic arm, in order to take advantage of its high precision displacement and repeatability capabilities (for further details, refer to the Mechanical Assembly section).

Extrusion system design The extruder design is composed of two chambers utilizing plunger actuation for viscous colloids and an additional chamber to handle dry or granular dispensing of natural fillers such as cellulose chopped fibers, fine sand, or natural polymer powders (Figure 1c). Bipolar stepper motors with noncaptive lead-screws (Figure 2d) linearly advance the materials to the tip by pushing the syringe plunger. The motors are mounted to CAD-CAM water-jet-cut aluminum frames that provide hardware support and vertical guides to prevent the lead-screws from

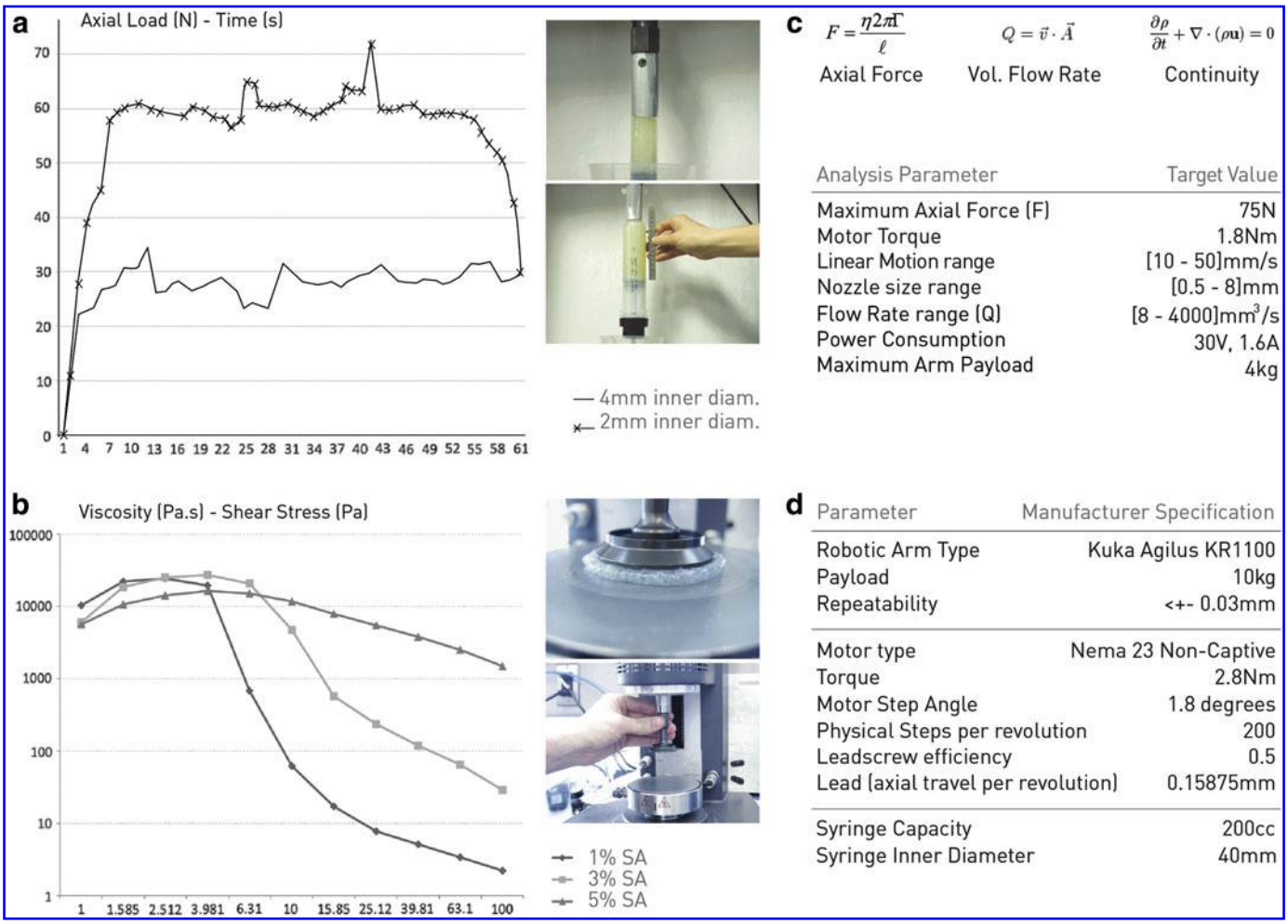

Figure 2. **(a)** Colloids tested in a 200cc syringe with a 40mm inner diameter, and a 4 and 2mm nozzle inner diameter. The sample requires an average axial load of 60 N to display a consistent flow rate. **(b)** Colloids tested under AR-G2 TA Instruments viscometer display shear thinning properties that improve extrusion of the material due to the presence of sodium alginate (SA) in the matrix. SA content in the matrix is tested at 1%, 3%, and 5% concentrations. **(c)** Initial calculations and volumetric flow rate physical testing provide insights to dimension the extrusion system for viscous colloids. **(d)** Summary of assembly capabilities and specifications. Color images available online at www.liebertpub.com/3dp

turning, thereby transmitting the rotor actuation force to linear motion.

Nozzle system design The system provides for the nozzles to be custom designed to step the 8 mm reservoir opening down to different diameters and material configurations for extrusion. For the samples presented here, we have designed and 3D-printed single nozzles with an inner diameter of 0.5, 0.7, 2, 3, and 4 mm that can be mounted at the end tips of other complex nozzles. We also designed a three-parallel-chamber nozzle with 2 mm final inner diameter, a tri-axial extrusion nozzle with 3 mm final inner diameter, and a three-material static mixing nozzle with 3 mm final inner diameter were also designed. Nozzle schematics are displayed in Figure 3.

Control and Operation

The desired objects were modeled in a computer-aided design platform, and custom code was written to slice surface-based geometry into layers, build a line-based tool path from curves, and stream the tool path steps to a central interface in the computer. The central interface computes input and output data from the design platform and to and from the mechanical parts of the system (robotic arm and extrusion stepper motors). Various machine paths were tested and evaluated for extrusion consistency and mechanical extrusion behavior starting with straight lines and moving into cylindrical paths and layered prismatic depositions. The tool paths are processed and transmitted to the robotic arm via a server socket, and to the motors via serial signal. Both output signals are synchronized for smooth control. The robotic arm sends back actual positions that can be compared with the targets sent for consistent coordinated feed/speed ratios. The interface takes into account forward and reverse motor drive to prevent material dripping. A stepper motor transmission code is developed that receives data from the central interface and sending signals to two driver boards that are set up to run the two-stepper motors simultaneously, thereby enabling variable extrusion rates and mixing ratios.

For the motor control hardware, a microcontroller board was used and bipolar drivers were powered through an external bench power supply at 30 V and 1.6 A in correspondence with the motor

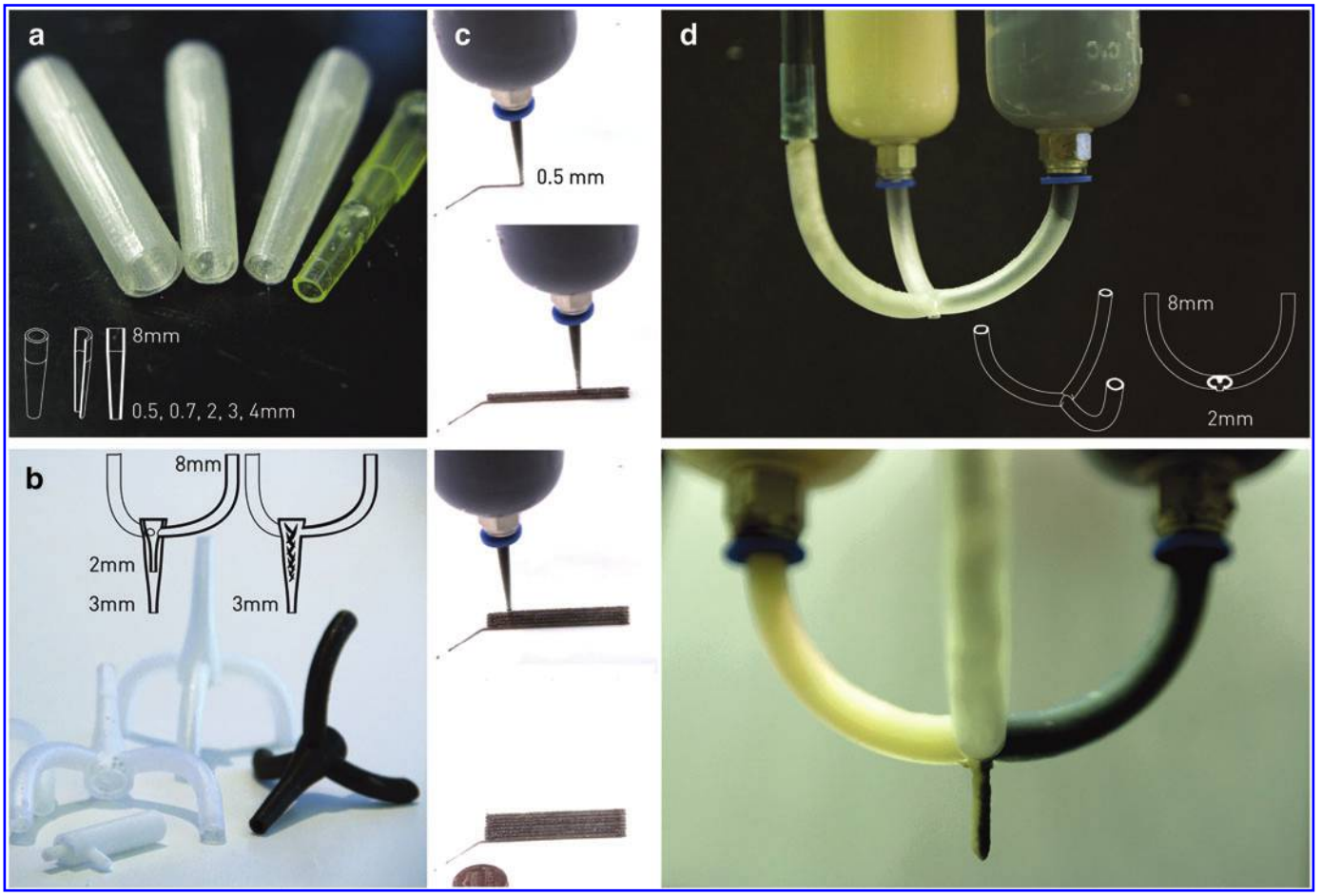

Figure 3. **(a)** Single-nozzle designs and tips. **(b)** Triaxial and static mixing nozzle designs. **(c)** Continuous extrusion with a single nozzle with 0.5mm feature size. **(d)** Parallel material extrusion nozzle depositing colloids mixed with white-and-black food coloring. (Nozzle line drawings indicate inner diameter measurements, are superimposed in their corresponding nozzle design photographs, and represented in perspective and section view.) Color images available online at www.liebertpub.com/3dp

MARY ANN LIEBERT, INC. • VOL. 1 NO. 3 • 2014 • DOI: 10.1089/3dp.2014.0014

specifications (see Materials and Methods for further details). Robotic movement and extrusion are not explicitly linked, which allows for independent control of each motor-driven syringe, and the displacement of the robotic arm end-effector. With the ability to vary each of these parameters individually in succession, there is more flexibility in the development of the tool as an experimental fabrication platform.

Materials and Methods

Material Characterization

Chitosan at 85% deacetylation, acetic acid, and sodium hydroxide pellets were purchased from Alfa-Aesar; sodium alginate was purchased from Melecule-R; chitin powder was purchased from NutriCargo LLC. The solution components were weighted using a 0.1 mg resolution analytical balance, model Mettler Toledo ML54 with 0.1 mg resolution and 0.2 mg linearity, are composed of chitosan 3% w/v in 1% acetic acid aqueous solution,[10,22,23] sodium alginate 4% w/v in 4% NaOH aqueous solution, and 16% chitin powder.[5]

Material Tests

The viscosity of 85% deacetylated chitosan is 20–300 cP, 1 wt. % in 1% acetic acid (at room temperature). In order to determine composite properties, oscillatory shear measurements were carried out at shear rates of 1–100 Pa over 10 min with a minimum normal force limit of 0.10 N and maximum of 50.00 N, to the chitosan 3% w/v with 1%, 3%, and 5% sodium alginate matrixes in an AR-G2 viscometer (TA Instruments) employing a cone aluminum geometry with a diameter of 60 mm, an angle of 2 degrees, and a shear rate of 28.6. All the measurements were performed at a constant temperature of 25°C; the AR-G2 viscometer has a transducer torque resolution of 1 nN·m, a maximum motor torque of 800 mN·m, a position accuracy of 0.1 μm, and a strain resolution of 0.04 μrad. The axial extrusion force tests were performed under an Instron mechanical tester with a 9071.85 kg (20.000 lb) reversible load cell, with a rated load/speed capability of 20.000 lb (10.000 kg, 100 kN) at speeds up to 50 mm/min (2.0 in./min) and a speed accuracy of ±0.1% of set speed at all loads and speeds, using a routine setup at a rate of 200 mm/min, sampling 120 times per minute and a load threshold of 500 N. Manufactured results were measured with a digital caliper model, Neiko Stainless Steel 152.4 mm (6 i.n) Digital Large LCD Display Caliper MM/SAE, with an accuracy of 0.0254 mm (0.001 in.).

Mechanical Assembly

The extrusion system was attached to an existing motion platform's end-effector. The existing platform is a Kuka KR AGILUS robotic arm (model KR 10 R1100 SIXX WP). The platform weighs 54 kg with a 10 kg payload and a maximum reach of 1101 mm. It has 6 axes, a $< \pm 0.03$ mm repeatability and employs the KR C4 compact control system. The stepper motors are equipped with noncaptive Acme lead-screws with 9.5 mm diameter and 635 mm length. For the single-nozzle assemblies, we used Oxford Universal plastic pipette tips of a 0.7, 1, and 2 mm inner diameter at the tip. For complex nozzle fabrication, we used the Formlabs Form1 SLS 3D printer with clear photo curable resin, 0.5 mm layer height, no internal support, and high exterior support density for maximum channel resolution to minimize extrusion calculation error due to material friction at the nozzle. For the mounting of the mechanical parts, we used 5 and 10 mm aluminum machinable sheets cut with a numeric control abrasive water-jet cutting machine (OMAX Corporation).

Hardware

A Mastech Linear DC power supply, model 30V 5A HY3005F-3, with triple outputs and dual adjustable outputs (0–30 V and 0–5 A) was used to power two bipolar motor stepper drivers Mondo Step 4.2, with an output current of 1–4.2 A, a supply voltage of 20–50 VDC, and a step frequency of 0–300 kHz. The bipolar noncaptive linear actuators, Haydon 57F4A, have a step angle of 1.8 degrees, a linear travel per step of 0.0079375 mm, and a force versus linear velocity of 1200 N at speeds below 1 mm/sec. The board where the system was controlled from an Arduino Mega 2560, with a computer-supplied input power of 5 V and an output power of 3.3 or 5 V, incorporating a high-performance, low-power Atmel AVR 8-Bit microcontroller.

Software

Geometric tool paths providing control and operation of the extrusion system were designed with Rhino3D modeling software (Rhinoceros; Robert McNeel and Associates) and its scripting plugin Grasshopper. Using the geometric kernel library of the plugin, custom C-sharp code was written to transmit fabrication instructions to the central interface. The central interface was written in C++ using the Eclipse IDE environment (2013 The Eclipse Foundation), which computes input and output data from the design platform to and from the mechanical parts. Transmission is achieved with an Ethernet UDP socket and via a serial USB signal. The stepper motor transmission code is developed in C code using the cross-platform open-source Arduino IDE (by Arduino Software).

Results

We expect that the water-based robotic fabrication technology presented in this article can enable the design, fabrication, and evaluation of sustainable products and building components. The technology enables the use of raw basic natural polymers, combined and diluted with low-impact chemicals and water, to deposit and cure products at room temperature, reducing and often omitting the requirement or need for external energy sources other than the mechanic extrusion and displacement of the nozzle. Using this technology, structural and material hierarchies can be designed and implemented to achieve multiple functionalities throughout the surface and volume area of the manufactured objects.

Layered Depositions

Initial material bonding and flow-rate consistency tests were performed, resulting in simple prisms (Figure 3c). Constructed $2 \times 1 \times 0.5$ cm prisms with a single-nozzle setup display minimum

feature sizes of 0.7 and 1 mm measured with a digital caliper of 0.0254 mm accuracy. Unidirectional and bidirectional tool paths were tested with significant improvement in layer bonding in the bidirectional samples (Figure 4a, b). Geometrically patterned tool paths with 0.7 mm thickness, displaying structural inertia when dried and detached from the substrate, were designed in anticipation of future development for object infill.

Parallel Depositions

Tests with a 3-chamber nozzle (using only 2 material chambers) display 2 mm feature size when two colloids with different coloration are extruded from the two actuated syringes. Figure 3c displays successful parallel extrusion of the materials. This interesting feature could be used in future work to deposit dual material geometries with different internal and external properties. This could avoid boundary de-lamination issues between the two materials, as the colloids are bond together while extruded through the multimaterial chamber at the nozzle. All samples were composed of chitosan–alginate matrix and chitin powder aggregate with white-and-black food coloring for visual contrast.

Graded Depositions

Material mixing at the nozzle provides for mechanical property variation within the samples, as well as for controlled material gradients with the intention of mimicking spatial organization and material composition strategies found in nature. Figure 5a displays the deposition process and result of a 30-cm-long design modeled after the maple seed. The structure obtains its inertia from chitosan–alginate reinforcement lines that follow the structural bending diagram of the construct. The clear color and tensile strength of the infill films are provided by a chitosan 3% interstitial filling. Figure 5b illustrates the deposition process and result of a 50-cm-long dragonfly wing design. The structure obtains its inertia from the cell pattern of chitosan–alginate reinforcement paths, and its tensile strength from chitosan 6% interstitial films. We have achieved deposition of chitosan concentrations from 1% to 10% w/v in 1% acetic acid solution through static mixing at the nozzle. When mixing the gels with a

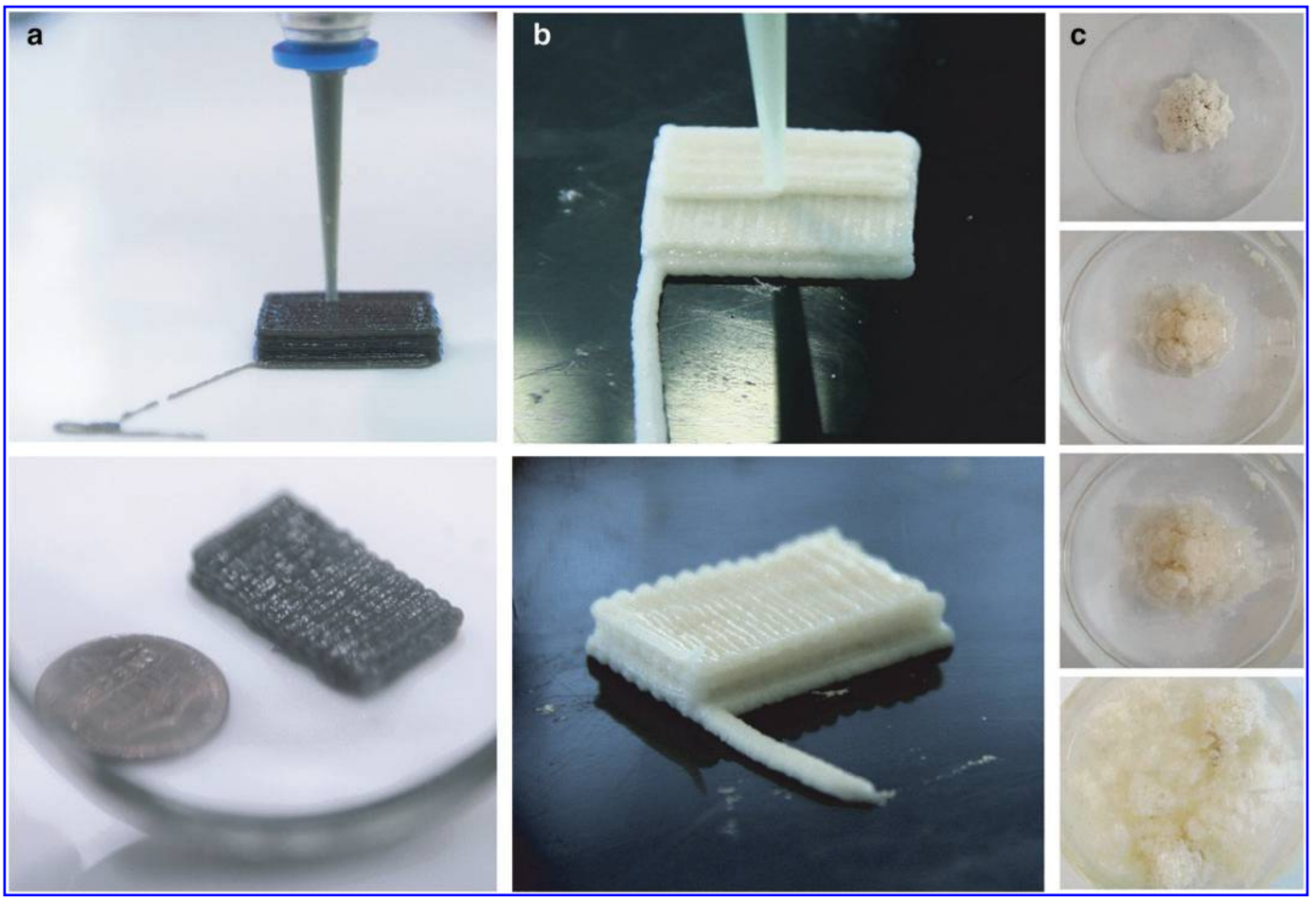

Figure 4. **(a)** A 2 × 1 × 0.5 cm prism printed using a 0.7 mm nozzle at 20 mm/sec printing speed to produce unidirectional layer orientations. The result is shown under a 1.5 augment magnifying lens in bottom column. **(b)** A 2 × 1 × 0.5 cm prism printed using a 0.7 mm nozzle at 20 mm/sec speed to produce bidirectional layer orientations. The result is shown in the bottom column. **(c)** A printed 15 g dried chitosan-based cone-shaped composite is dissolved at room temperature in 200 ml of water over 20 min, demonstrating colloids biodegradability. Color images available online at www.liebertpub.com/3dp

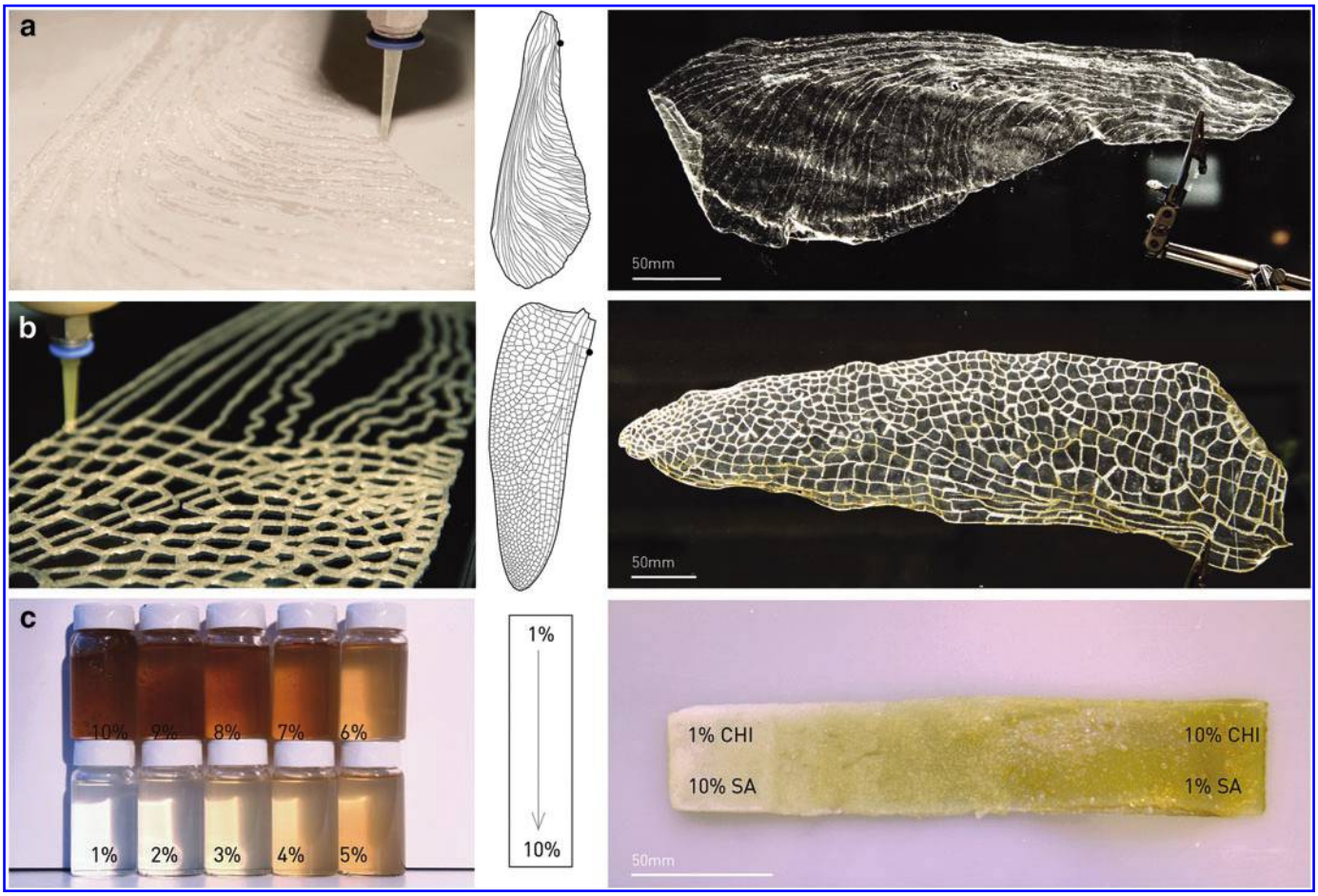

Figure 5. **(a)** Water-based deposition of a 30-cm-long material patch modeled after the maple seed. The patch exhibits reinforcement trajectories aligned with the form's anticipated structural bending. **(b)** Water-based deposition of a 50-cm-long material patch modeled after the dragon *y* wing. The patch exhibits structural inertia. **(c)** Chitosan concentrations range from 1% to 10% w/v in 1% acetic acid solution. Gradient chitosan concentrations are statically mixed at the nozzle with sodium alginate as a thickening agent. Both sodium alginate content and chitosan concentration differences also provide for optical density variation. The gradient ranges from 11% aggregate, 1% chitosan (CHI), and 10% sodium alginate (SA), to 10% chitosan (CHI) and 1% sodium alginate (SA). Color images available online at www.liebertpub.com/3dp

sodium alginate thickening agent, we achieve viscosities with deposition-compatible properties still displaying the optical density qualities of the gels. In Figure 5c the deposited range contains a gradient of concentration and of thickening agent: from 1% chitosan and 10% sodium alginate to 10% chitosan and 1% sodium alginate.

Biodegradability

We have evaluated whether a 15 g conical prototype of 30-mm-diameter base and 30 mm height put to dry overnight will dissolve in 200 ml of water at room temperature after 20 min (Figure 4c). The samples can have longer stability to moisture by submerging them in a 4% NaOH w/v aqueous solution for 5 min once dried, and then dried again overnight. Nevertheless, chitosan–alginate composites will biodegrade over time when exposed to the environment. This capability can be used to design temporary and highly ecological architectural-scale parts that can interact with the environment by contributing to soil nutrient levels over time during decay. Plant growth on a 40-mm-diameter and 8-mm-height disc of mixed chitosan and plant soil was tested with grass seeds growing over a week with no loss of disc consistency or integrity.

Conclusions

A wide variety of raw biodegradable materials exist in nature that display structural and environmental properties superior to those currently used for mass production of commercial products.[3] However, research into AM processes for sustainable structures is still in its infancy, specifically in disciplines such as product engineering, product design, and architectural design. Chitin, alginate, and their respective chitosan and sodium alginate derivatives are responsible for some of the most remarkable mechanical properties exhibited by natural materials, including seaweed gum, nacre, insect cuticle, and crustacean shells, and are as abundant on earth as cellulose, the main constituent of cotton or wood.[1,2,10]

In nature, water provides for invisible support, and its function is structural, mediating between the internal

chemistry and the external environment. We have presented water-based robotic fabrication as the combination of chitosan and sodium alginate hydrogel matrixes with other organic aggregates, to deposit biodegradable prototypes using mechanically actuated extrusion methods. We have demonstrated the approach by building and testing the mechanics and controls of a multichamber portable extrusion system that can be attached to numeric control multiaxes platforms. The utility of the system was demonstrated by fabricating depositions of natural composite-material objects. Preliminary results display consistent volumetric flow rates, submillimeter to macroscale features, and graded properties. Water-based robotic fabrication holds potential applications for fully recyclable products or architectural parts with graded mechanical, optical, and environmental properties such as water storage, hydration-induced shape change, or full disintegration over time.

Future research is currently under way in our group to improve the prototype by designing an actuated mixing system at the nozzle with a helical screw, instead of a static mixing one, where full combination of the materials is more precisely ensured. We also envision the design of a servo-actuated gravity feed for the syringe containing dry or granular materials. In addition, we are actively investigating the implementation of a pneumatic extrusion system (using air pressure and solenoid valves), instead of the current volume-driven system (using stepper motors), that could provide for the generation of more complex extrusion paths. In terms of further material explorations, cellulose chopped fibers should be tested to provide enhanced mechanical properties of printed objects. In terms of advanced controls: mechanical property prediction models should be integrated to inform the variations of geometrical and chemical design of the objects.

We anticipate that the approach and enabling technology presented in this article will contribute to the field of sustainable AM of biodegradable material systems. The technology enables the deposition of functionally graded constructs with structural hierarchies made of basic building blocks and processed via water and low-impact chemicals. The technology enables the deposition and curing of constructs at room temperature, with no external energy sources other than mechanical extrusion and displacement of the nozzle.

Acknowledgments

This research was primarily sponsored by the Mediated Matter research group at the MIT Media Lab and in part by the MIT Department of Mechanical Engineering through a project in the course Additive Manufacturing (2.S998) in Spring 2014. Ideas, methods, products, and techniques were developed to support an ongoing group project and research platform focusing on biodegradable AM commissioned by the TBA-21 Academy (Thyssen-Bornemisza Art Contemporary). We would like to thank Associate Prof. John A.Hart, Alfonoso J. Perez, and Jamison Go for their support of our work and for their technical advice. We would also like to thank Dr. Javier Fernandez and Dr. James Weaver from the Wyss Institute at Harvard University for their guidance and support. We thank Pierce Hayward and Alexander Barbati for their assistance in material characterization tests in the MIT Mechanical Behavior of Materials Lab and the MIT Fluids Lab. In addition, we wish to thank our colleagues from the MIT Media Lab, Jared Laucks, Markus Kayser, Steven Keating, and Arthur Petron, for their assistance with mechanical designs. Finally, we thank our UROP team for their continuous support of this project, including Daniel Lizardo, Selda Buyukozturk, Dimitrios Pagonakis, Tina Zheng, Grace Young, and Maya Sathaye.

Author Disclosure Statement

No competing financial interests exist.

References

1. Fernandez JG, Ingber DE. Manufacturing of large-scale functional objects using biodegradable chitosan bioplastic. Macromol Mater Eng 2014;299:932–938.
2. Fernandez JG, Ingber DE. Bioinspired chitinous material solutions for environmental sustainability and medicine. Adv Funct Mater 2013;23:4454–4466.
3. Ashby MF, Gibson LJ, Wegst U, et al. The mechanical properties of natural materials. I. Material property charts. Proc Math Phys Sci 1995;450:123–140.
4. Dumitriu S. Polysaccharides: Structural Diversity and Functional Versatility. Marcel Dekker, New York, NY, 2005.
5. Li Z, Ramay HR, Hauch KD, et al. Chitosan-alginate hybrid scaffolds for bone tissue engineering. Biomaterials 2005;26:3919–3928.
6. Geng L, Feng W, Hutmacher DW, et al. Direct writing of chitosan scaffolds using a robotic system. Rapid Prototyping J 2005;11:90–97.
7. Rinaudo M. Chitin and chitosan: Properties and applications. Progr Polym Sci 2006;31:603–632.
8. Vincent JFV. Structural Biomaterials. Macmillan, London, 2012.
9. Miserez A, et al. The transition from stiff to compliant materials in squid beaks. Science 2008;319:1816–1819.
10. Fernandez JG, Ingber DE. Unexpected strength and toughness in chitosan-fibroin laminates inspired by insect cuticle. Adv Mater 2012;24:480–484.
11. Oxman N. Variable property rapid prototyping. Virtual Phys Prototyping 2011;6:3–31.
12. Holshouser C, et al. Out of bounds additive manufacturing. Adv Mater Processes 2013. www.osti.gov/scitech/servlets/purl/1068744 (last accessed June 2014).
13. Voxeljet. VXC800: The continuous 3D printer. http://goo.gl/Ha2NjQ (last accessed June 2014).
14. D-Shape: The technology. http://goo.gl/oUK2GC (last accessed June 2014).
15. Stratasys. Objet1000: Build full-scale prototypes in multiple materials. http://goo.gl/DYzWxy (last accessed June 2014).
16. Sherman LM (Plastics Technology). Additive manufacturing: Materials for real-world parts. http://goo.gl/gR6e0S (last accessed June 2014).
17. Hiller J, Lipson H. Design and analysis of digital materials for physical 3D voxel printing. Rapid Prototyping J 2009;15:137–149.

18. NASA. NASA's EBF3: The future of art-to-part manufacturing. http://goo.gl/irfmfJ (last accessed June 2014).
19. ARUP. Construction steelwork makes its 3D printing premiere. http://goo.gl/QQbpib (last accessed June 2014).
20. Kieback B, Neubrand A, Riedel H. Processing techniques for functionally graded materials. Mater Sci Eng 2003;362:81–106.
21. Omenetto FG, Kaplan DL. New opportunities for an ancient material. Science 2010;329:528–531.
22. Melchels FPW, Domingos MAN, Klein TJ, et al. Additive manufacturing of tissues and organs. Progr Polym Sci 2011;37:1079–1104.
23. Gutowska A, Jeong B, Jasionowski M. Injectable gels for tissue engineering. Anat Rec 2001;263:342–349.
24. Malda J, Visser J, Melchels FP, et al. 25th anniversary article: Engineering hydrogels for biofabrication. Adv Mater 2013;25:5011–5028.
25. Billiet T, Vandenhaute M, Schelfhout J, et al. A review of trends and limitations in hydrogel-rapid prototyping for tissue engineering. Biomaterials 2012;33:6020–6041.
26. Malone E, Lipson H, Fab@Home the personal desktop fabricator kit, Rapid Prototyping Journal, 2007;4:245–255.

Address correspondence to:
Neri Oxman
MIT Media Lab
75 Amherst Street, E14-433B
Cambridge, MA 02139

E-mail: neri@mit.edu

This article has been cited by:

1. Shannon E. Bakarich, Robert Gorkin, Reece Gately, Sina Naficy, Marc in het Panhuis, Geoffrey M. Spinks. 2017. 3D printing of tough hydrogel composites with spatially varying materials properties. *Additive Manufacturing* **14**, 24-30. [CrossRef]
2. Sandeep S. Ahankari, Kamal K. KarFunctionally Graded Composites: Processing and Applications 119-168. [CrossRef]
3. Ibrahim T. OzbolatExtrusion-Based Bioprinting##With minor contributions by Monika Hospodiuk, The Pennsylvania State University 93-124. [CrossRef]
4. Xiao Li, Qin Lian, Dichen Li, Hua Xin, Shuhai Jia. 2017. Development of a Robotic Arm Based Hydrogel Additive Manufacturing System for In-Situ Printing. *Applied Sciences* **7**:1, 73. [CrossRef]
5. Liao Chao-Yaug, Wu Wei-Jen, Hsieh Cheng-Tien, Tseng Ching-Shiow, Dai Niann-Tzyy, Hsu Shan-hui. 2016. Design and Development of a Novel Frozen-Form Additive Manufacturing System for Tissue Engineering Applications. *3D Printing and Additive Manufacturing* **3**:4, 216-225. [Abstract] [Full Text HTML] [Full Text PDF] [Full Text PDF with Links]
6. Ibrahim T. Ozbolat, Monika Hospodiuk. 2016. Current advances and future perspectives in extrusion-based bioprinting. *Biomaterials* **76**, 321-343. [CrossRef]
7. Monika Hospodiuk, Kazim Kerim Moncal, Madhuri Dey, Ibrahim T. OzbolatExtrusion-Based Biofabrication in Tissue Engineering and Regenerative Medicine 1-27. [CrossRef]
8. Yao Lining, Ou Jifei, Wang Guanyun, Cheng Chin-Yi, Wang Wen, Steiner Helene, Ishii Hiroshi. 2015. bioPrint: A Liquid Deposition Printing System for Natural Actuators. *3D Printing and Additive Manufacturing* **2**:4, 168-179. [Abstract] [Full Text HTML] [Full Text PDF] [Full Text PDF with Links]